Global Journal of Engineering and Technology Advances
eISSN: 2582-5003
Cross Ref DOI: 10.30574/gjeta
Journal homepage: https://gjeta.com/

(Research Article)

Check for updates

Evaluation of the physical and mechanical properties of Al-Zn-Mn alloys manufactured from recycled aluminum wire

Tamer Khalil MohammedAli [1,*], Adnan Raad Ahmed Ali [1] and Mahmood Ahmed Hmod [2]

[1] *Department of Physics, University of Tikrit, College of Education for pure Science, Tikrit, Iraq.*
[2] *Department of Physics, University of Mosul, College of Science/Mosul, Iraq.*

Global Journal of Engineering and Technology Advances, 2023, 15(02), 060–072

Publication history: Received on 05 a 2023; revised on 16 May 2023; accepted on 19 May 2023

Article DOI: https://doi.org/10.30574/gjeta.2023.15.2.0089

Abstract

Aluminum wire scrap was collected to manufacture ingots, as we melted aluminum wires with high purity zinc and manganese metal. To examine the physical and mechanical properties, these alloys were cut into small strips and polished. The Vickers hardness (HV) technique was used to measure the hardness. The mechanical properties of the alloy increased with increasing zinc and manganese concentrations. It is observed that the values obtained from the EDX measurements and the SEM images are identical. Ingots contain gray and black areas; In the black region found, the elemental ratios of Al and Mn are high. XRD analyzes show that the α-Al peak is the main peak of all alloy configurations shown in all alloys. The secondary phases are Al2Mn and Al(MnZn) 6. It is clear that when the percentage of zinc increases, the parameters in the alloy structure decrease.

Keywords: Recycling of Aluminum; Aluminum wire; Mechanical properties; Structure properties; Al alloys

1. Introduction

Everyone can see aluminum everywhere. It can be found in foil, food packaging, beverage cans, automobile components, and other things. Aluminium alloys are currently in greater demand in the transportation sector. This is partially a result of efforts to reduce the weight of cars. Also, introducing electric vehicles and financial pressure on the automotive sector request decreased production costs. More specifically, the dynamics and competition in the transportation sector are the main forces behind the ongoing development of less expensive, novel, and creative materials applications[1]. The ability of aluminum to be recycled repeatedly with no harm to its quality and with little material loss due to oxidation (1-2) % may be its most important characteristic. Recycling aluminum saves 95% more energy and emissions than ore, essential in an environment with carbon restrictions[2]. Recycled aluminum, in particular, is increasingly used in automotive applications, which is crucial since it decreases vehicle mass, stabilizes fuel efficiency, and reduces pollutants. Nowadays, it is anticipated that this application will reduce the aluminum industry's carbon footprint. Aluminum and its alloys offer a very wide range of abilities and applications. Unique combinations of features of aluminum and its alloys make aluminum one of the most versatile, economical and attractive metallic materials for a wide range of uses from highly resilient soft laminates to the most demanding engineering applications [3].

Here are some of the unique specifications of this mineral : Aluminum has a density of about 2.7 g/cm^3, approximately one-third as much as steel (7.83 g/cm^3). Such lightweight, coupled with the high strength of some aluminum alloys (exceeding that of structural steel), permits the design and construction of strong, lightweight structures that are particularly advantageous for anything that moves-space vehicles and aircraft as well as all types of land- and water-borne vehicles. An exceptional characteristic of aluminum is its recyclability without losing physical and chemical properties [4]. This makes the metal an excellent choice, especially for the protection, storage and preparation of food and beverages. Aluminum can be rolled into ultra-thin foils, which are light, and strong and have unusual barriers and

* Corresponding author: Tamer Khalil MohammedAli

insulation qualities to preserve food and beverages against ultraviolet light and bacteria. Aluminum packages are secured, tamper-proof, hygienic, easy to open and recyclable. Almost every aluminum product that is produced commercially can be recycled after its end of life, without losing its metal properties or quality. As there is the increased use of recycled aluminum in many kinds of applications, aluminum metal is also known as green metal [5].

The growth in recycled metal becoming available is a positive direction, as secondary metal produced from recycled metal requires only about 2.8 kWh/kg of metal produced. In comparison, primary aluminum production requires about 45 kWh/kg of metal produced. It is to the industry and national advantage to maximize the amount of recycled metal, both from the energy savings and reduction of dependence upon overseas sources. And also, from the ecological standpoint, since recycling emits only about 4% as much CO_2 as primary production[6]. This study aims to produce new alloys by recycling wire of aluminium high purity with adding zinc and manganese metal. The mechanical and physical properties are testing of these alloys.

2. Material and method

The effect of the zinc and manganese elements on aluminium-based alloys is investigated in this work. Based on this, we used the smelting method to produce samples with different ratios of elements. The metals and devices used to complete this research have been prepared, and they are as follows: The collection of scrap aluminum alloy as aluminum wires used in the transmission of electric power, which are considered to be of high purity, high purity zinc metal and manganese metal each with purity 99.99%.

In this work, we primarily concentrated on ternary alloys (X-Y-Z alloy, where X, Y, and Z are Al, Zn, Mn). these alloys were produced by casting method. Atomic and weight percentages of X-Y-Z alloys (X, Y, Z: Al, Zn, Mn) with different atomic percentages, concentrations of alloys is calculated by Equation (1).

$$\text{The Ratios of alloys \%} = \frac{at1 + at2 + at3}{100} \text{ ------------- (1)}$$

Where:
At : weight percentages of elements

The alloys were produced by recycling aluminium wire and adding different weight ratios of zinc and manganese, as seen in Fig.1. The metal powders are combined with aluminum scrap, and a smelting process is carried out in a gas furnace. The mixing process was carried out more than once to achieve the required homogeneity. The first objective was to make a 25-gram ingot for which the proportions of its components were calculated according to equation (1).

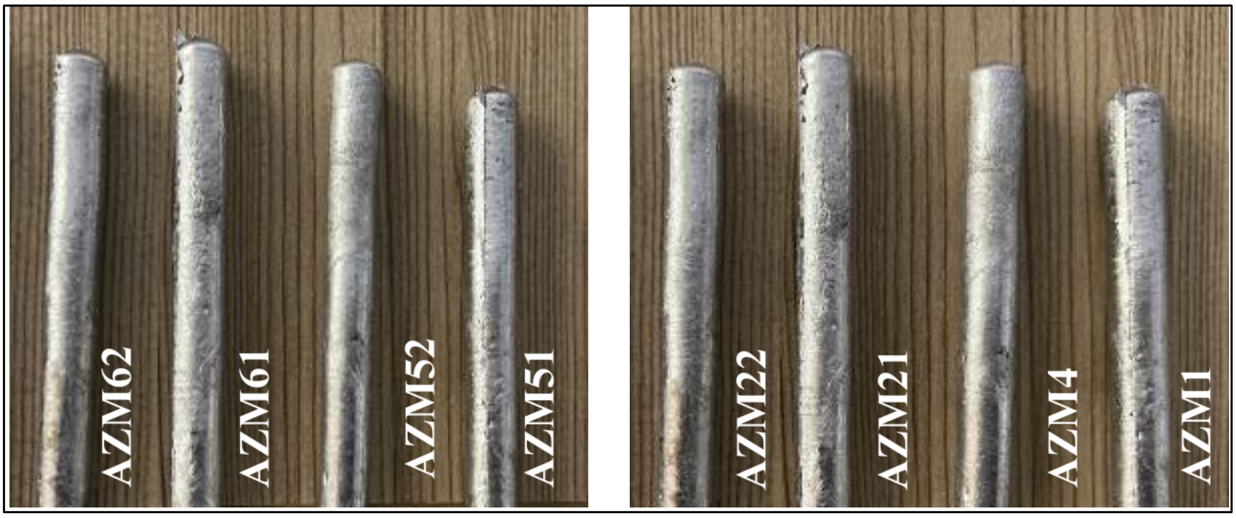

Figure 1 Examples of the resulting shaped alloys

Heat treatments are used to improve the alloy's structural properties. Therefore, heat treatment is applied to the produced alloys after the smelting process. The alloys were wrapped in aluminum foil and heated to 300 °C for 1 hour in an electric furnace. The ingots were subjected to 24-hour slow cooling at room temperature. After heat treatment, the alloys were cut and polished using metal cutting and polishing equipment to perform physical and mechanical tests. The alloys' lattice properties were established using an X-ray diffractometer. The Energy Distribution Spectroscopy (EDX) method was used to calculate the alloy ratios. Scanning electron microscopy (SEM) was used for microstructural analyses. Using the EDX system, compositional analyses, SEM analyses, and mapping analyses of alloys were performed.

For mechanical Measurements applying the compression and hardness measurements. The Hardness Vickers (HV) technique of measuring hardness is used and is represented by the following equation [7][8][9][10]:

$$HV = 2\,P\,sin(\emptyset/2)/(D^2_{mean}) = 1.854\ P/(D^2_{mean}) \text{ --------------- } (2)$$

where:
HV: measurement of Hardness Vickers,
P : is the load in (kg),
$\boldsymbol{\emptyset}$ = 136º, $\sin\left(\frac{\emptyset}{2}\right)$= 0.927
$\boldsymbol{D^2}$: is the squared average between the length and width of pressured diamond head .

Additional hardness metrics are computed as well. Brinell Hardness (HB) has been evaluated by equation at bellow

$$\frac{x_1}{y_1} = \frac{x_2}{y_2} \text{ ------------------------- } \quad (3)$$

Where:
x_1 *and* x_2 from hardness conversion table is HV (Hardness Vickers measurement) and
y_1 *and* y_2 is Diameter from diamond head's length and breadth.

The simple formula for calculating (Tensile Strength) TS is as follows [7]:

$$TS=3.45 \times HB \text{ ,, } (4)$$

Where:
TS stands for Tensile Strength and HB for Hardness Brinell.

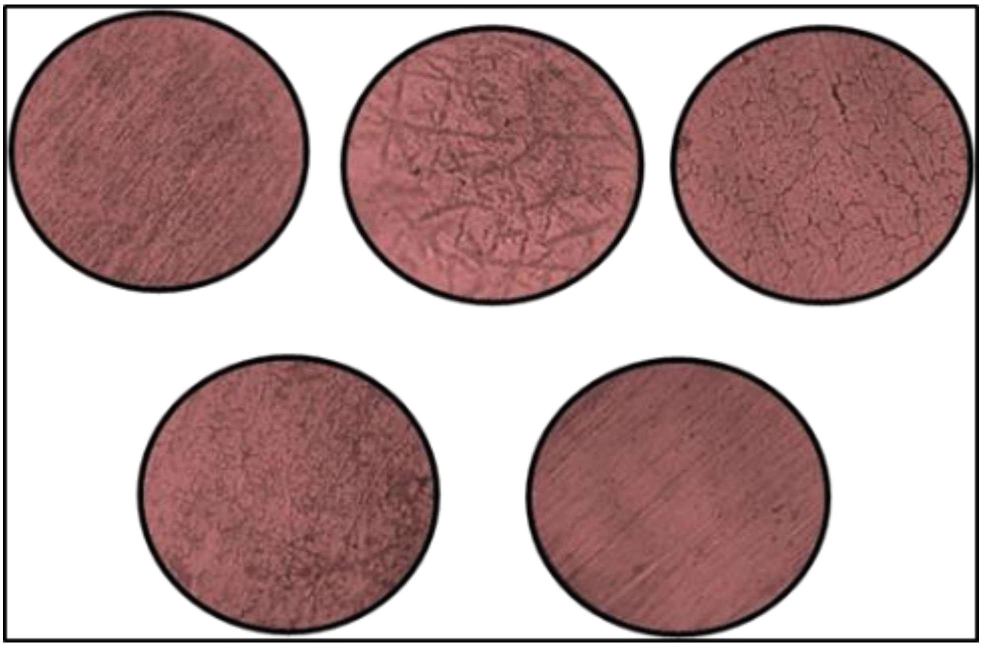

Figure 2 Examples of captured for structures of some alloys

3. Results and discussion

3.1. X-Ray Analyses

X-ray investigation of samples using the computer-controlled Rigaku RadB-DMAX II X-ray diffractometer and CuK radiation (λ = 1.5405 Å), measurements 2θ It was taken between 20° and 80° at a constant scanning rate of 2°/min at room temperature.

The structure can be determined based on the element ratios of the samples obtained. The secondary phases of Al_2Mn phase, as well as Mn (with a dominant hcp base structure), are recognized as the matching peaks [5]. The element ratios of the samples can be used to identify the structure. The corresponding peaks are identified as the secondary phases of the Al_2Mn phase and Mn [5].

According to the element ratios of the samples obtained, information about the structure of alloys can be obtained. Peaks in the XRD data of the alloys, which show the structural determinants of the alloys. The secondary phases Al2Mn phase and $Al(MnZn)_6$ phase, as well as Al (dominating hcp base structure), are identified as the peaks that match. At room temperature, it can be seen that the parameters in the alloy sample structure decrease as the Zn content increases [11][12].

After the obtained alloys are subjected to heat treatment, the X-ray measurement of the sample is 2^o/min. It was done with scanning speed between $(20 – 80)^o$. The X-Ray diffractogram of the Al-Mn-Zn alloys taken at room temperature is also given in Figures (3 and 4) .Microstructural characterization of the ternary alloys under study revealed the presence of dendrites with small precipitates in the alpha-Al matrix. α-Al peak is visible at all alloy structures. Figures (3 and 4).The observed peaks in the reflections shown in the figures of X-ray diffractogram, which are in agreement with literature. The reflections showed that the plane of about 39^o α-Al had the highest reflection in all alloys. Each alloy, the peak values, and the corresponding degrees in the figures are presented in a table (1). These results are consistent with the results of the literature [13].

Table 1 XRD Analysis for Al-Zn-Mn alloys

	Code of alloys	Weight present (% wt) (gm)			The X-Ray diffractogram information	
		Al	**Zn**	**Mn**	**Phases**	**2θ degree**
1	AZM62	18	1	6	α-Al	39^o, 46^o, 79^o
					Al_2Mn	76^o
					$Al_{18}(MnZn)_7$	37^o
					Zn	44^o
2	AZM61	18	1	6	α-Al	39^o, 45^o, 66^o, 79^o
					Al_2Mn	54^o, 75^o
					$Al_{18}(MnZn)_7$	42^o , 47^o
					Zn	37^o
3	AZM52	18	2	5	α-Al	39^o, 46^o, 66^o, 79^o
					Al_2Mn	42^o, 76^o
					$Al_{18}(MnZn)_7$	44^o, 58^o
					Zn	26^o, 37^o
4	AZM51	18	2	5	α-Al	39^o, 45^o, 79^o
					Al_2Mn	42^o, 46^o, 66^o
					$Al_{18}(MnZn)_7$	43^o, 47^o
					Zn	-

5	AZM22	18	5	2	α-Al	39°, 46°, 79°
					Al_2Mn	37°, 66°
					$Al_{18}(MnZn)_7$	45°
					Zn	22° , 55°
6	AZM21	18	5	2	α-Al	38°, 46°, 66°, 79°
					Al_2Mn	44°
					$Al_{18}(MnZn)_7$	37°, 46°
					Zn	55°, 71°
7	AZM4	18	3	4	α-Al	39°, 45°, 66°, 78°
					Al_2Mn	44°, 71°
					$Al_{18}(MnZn)_7$	37°, 51°, 71°
					Zn	32°
8	AZM1	18	6	1	α-Al	39°, 45°, 66°, 79°
					Al_2Mn	36°, 44°
					$Al_{18}(MnZn)_7$	37°, 71°
					Zn	54°

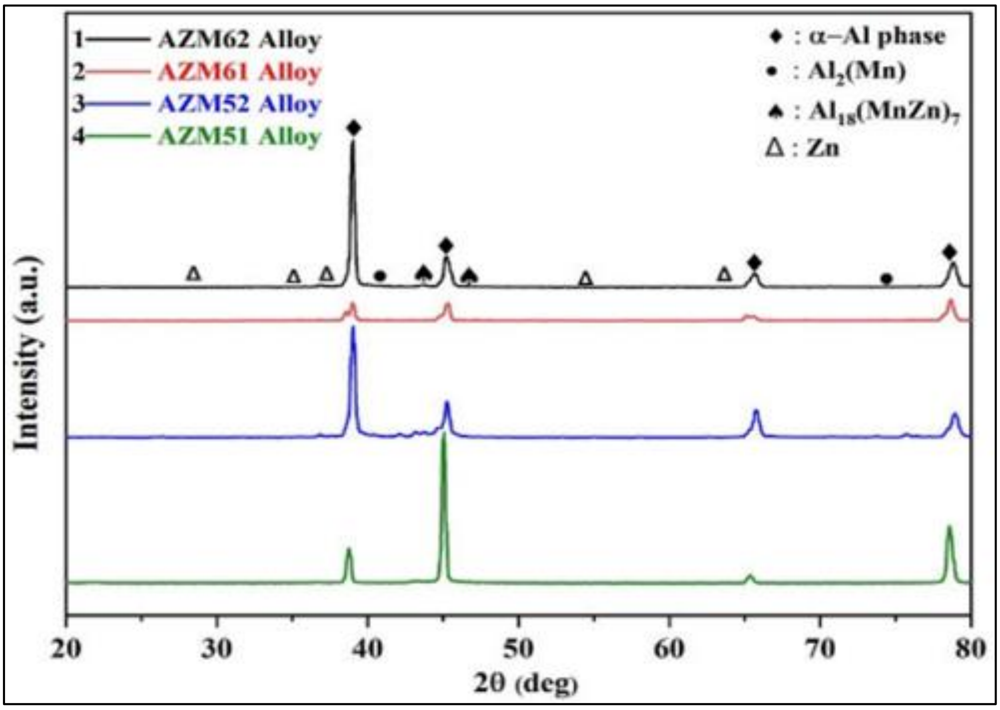

Figure 3 X-ray diffractogram of the (AZM62, AZM61, AZM52 and AZM51) alloys sequentially

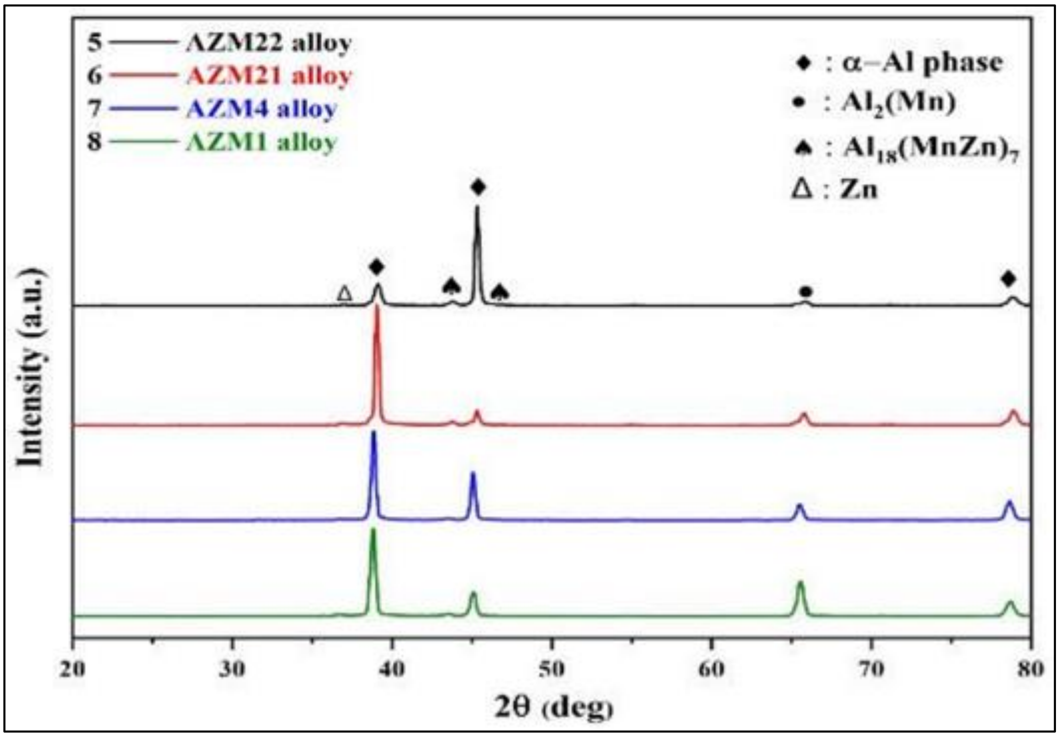

Figure 4 X-ray diffractogram of the (AZM22, AZM21, AZM4 and AZM1) alloys sequentially

3.2. EDS Invistigation

Following the alloys' heat treatment, the samples were cut into pieces using a small metal cutting device for SEM-EDS analysis. A polishing tool was used to polish the slices of alloys after they had been implanted in polyester resin. The polished surface was etched using a 75ml HCl, 75ml ethanol, 15g $CuSO_4$, and 10ml distilled water etching solution. Etching was followed by the capture of optical micrographs and SEM pictures. SEM images of the alloy surface and its various regions have been collected. Many regions were chosen for the EDS spectra in order to calculate the weight and atomic percent ratio of the alloys. The results are presented in Table (2) based on the alloy concentration. Accourdıng to EDS results, The alloys' percent weight and atomic values differ when the EDS spectrum data are compared to the ratios established before casting. Although the samples were kept far from oxidation but oxidation nevertheless took place as the elements melted and turned into powder. Because some slag was created as a result of oxidation, the ratios before casting and after casting were different from one another.

Al, Zn, and carbon are all present in sizable concentrations, according to the EDS spectra. The oxygen content is present in both the Al-Mn-Zn. The EDS spectra of Al-Mn-Zn include oxygen, further demonstrated that the Mn is present in the form of an oxide. According to the EDS, these values indicate that all of the chemical precursors of Al-Mn-Zn alloy alloys were equally and completely distribution through the surface of alloys. The presence of aluminum and manganese causes the creation of MnAl inclusions, as indicated in the SEM image Figure (5), and this is verified by the EDS spectra acquired at specific sites, as the manganese element is not visible in some regions. This results agreement with Khin Sandar [14].

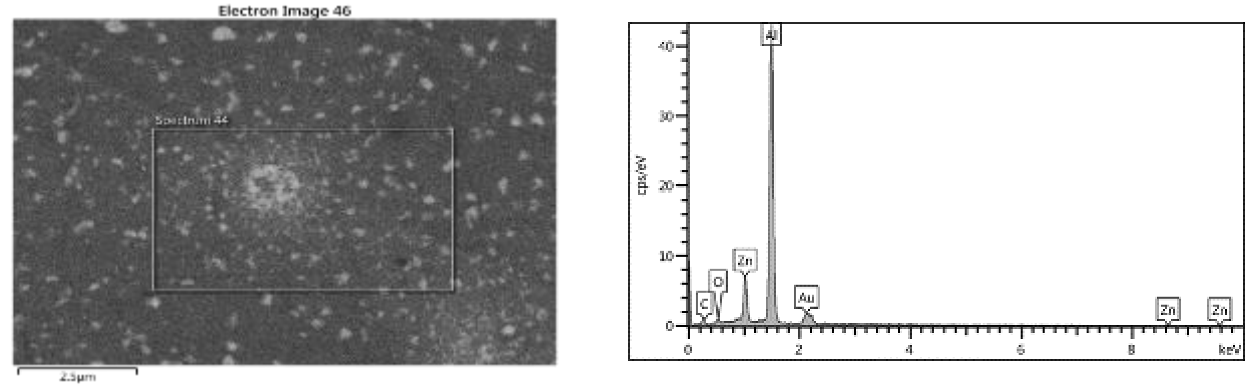

(AZM4)

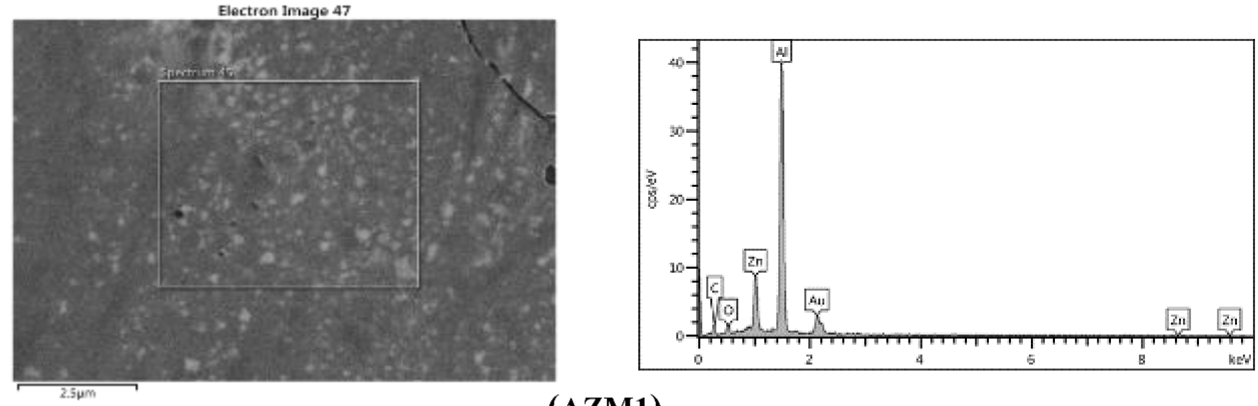

(AZM1)

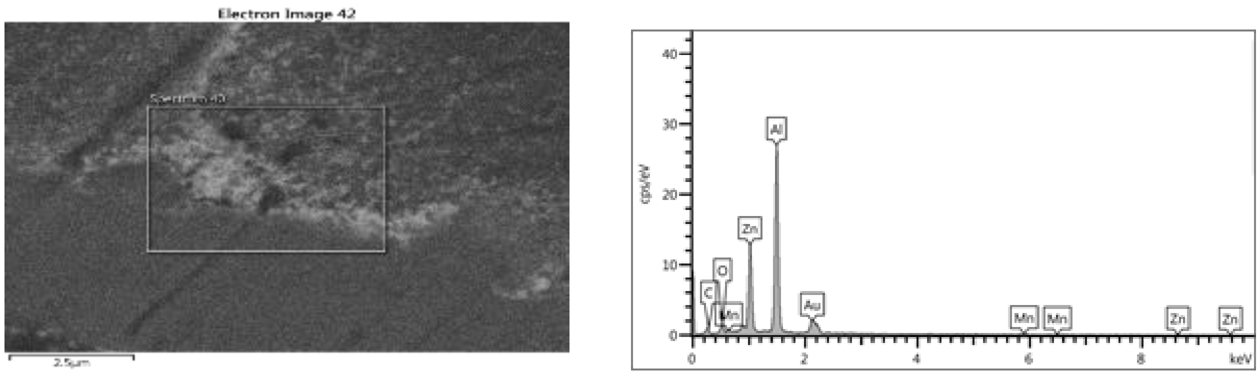

(AZM52)

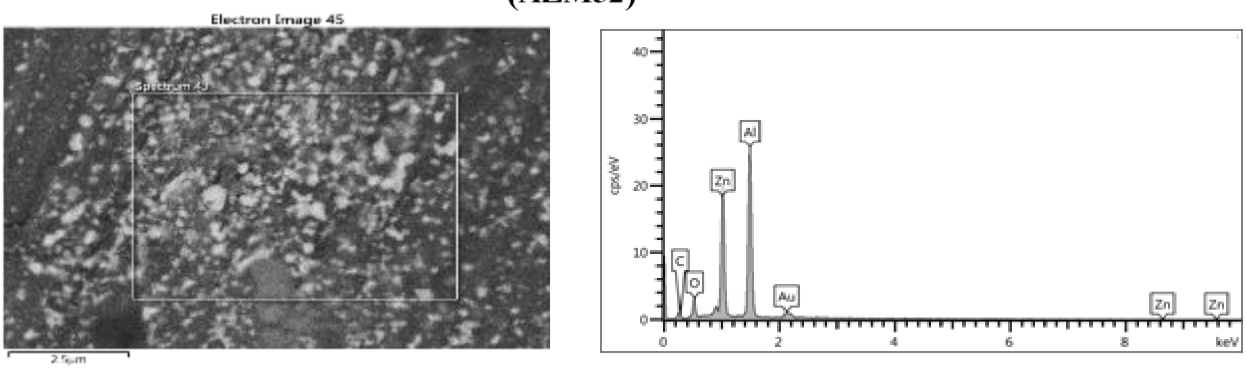

(AZMg3)

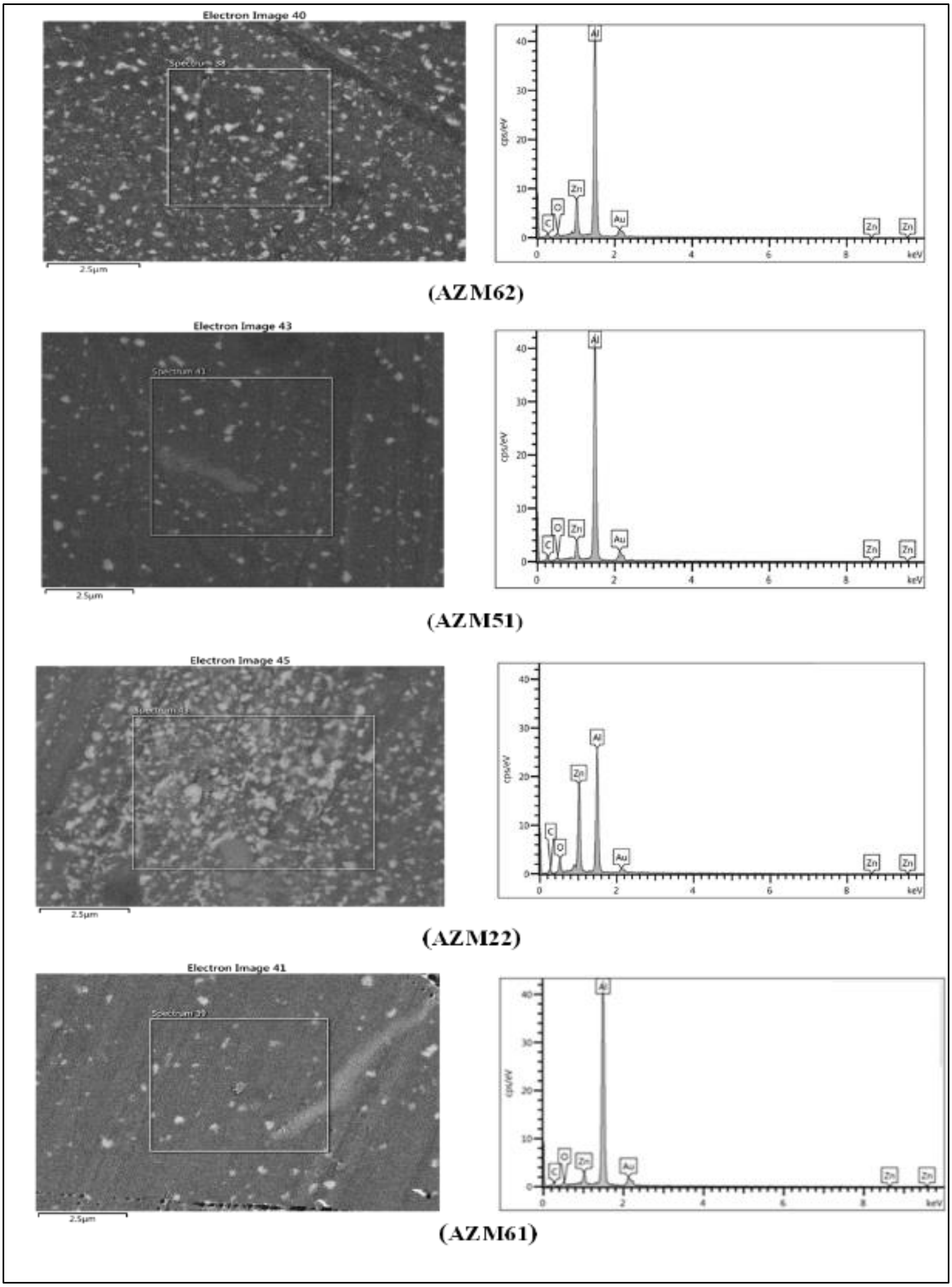

Figure 5 The image of ternary alloys by electron micro analysis at the surface of specimens using energy-dispersive spectroscopy (EDS)

Table 2 Element ratios obtained by EDS analysis results of Al-Zn-Mn alloys

Code of alloys		Weight percent(% wt) (gm)			(% atomic) by EDS		
		Al	**Zn**	**Mn**	**Al**	**Zn**	**Mn**
1	AZM62	18	1	6	77.7	18.9	-
2	AZM61	18	1	6	88.9	7.0	-
3	AZM52	18	2	5	57.2	35.3	2.0
4	AZM51	18	2	5	85.0	10.5	-
5	AZM22	18	5	2	67.2	30.0	-
6	AZM21	18	5	2	47.7	45.3	-
7	AZM4	18	3	4	80.7	15.6	-
8	AZM1	18	6	1	72.6	20.6	-

3.3. SEM analysis of alloys

For the purpose of polishing and etching the alloys, a chemical etching solution (75ml HCl, 75ml ethanol, 15g $CuSO_4$ and 10ml distilled water) was applied. After the samples were etched, the surfaces were captured in SEM images. Images were taken from the same region for each sample at varied magnifications.

The formation of Al_2Mn components is caused by the presence of aluminum and manganese, as shown in the SEM image Figure (6), and agreed by the EDX spectral data obtained at designated regions. The results were in perfect agreement with the XRD spectrum. Phase peaks are also seen in the X-ray diffractogram. The alloys show a basic microstructure with alpha-Al, in addition to the Al2Mn phase in (Al-Mn-Zn) alloys and Al_2Mg phases in (Al-Zn-Mg) alloys.

Figures (6) show that the single-phase and two-phase zones are denoted by grey and black areas respectively. Al and Mn element ratios were found to be high in the black zones. These results was agreement with the values obtained from the EDX measurements and the SEM images.

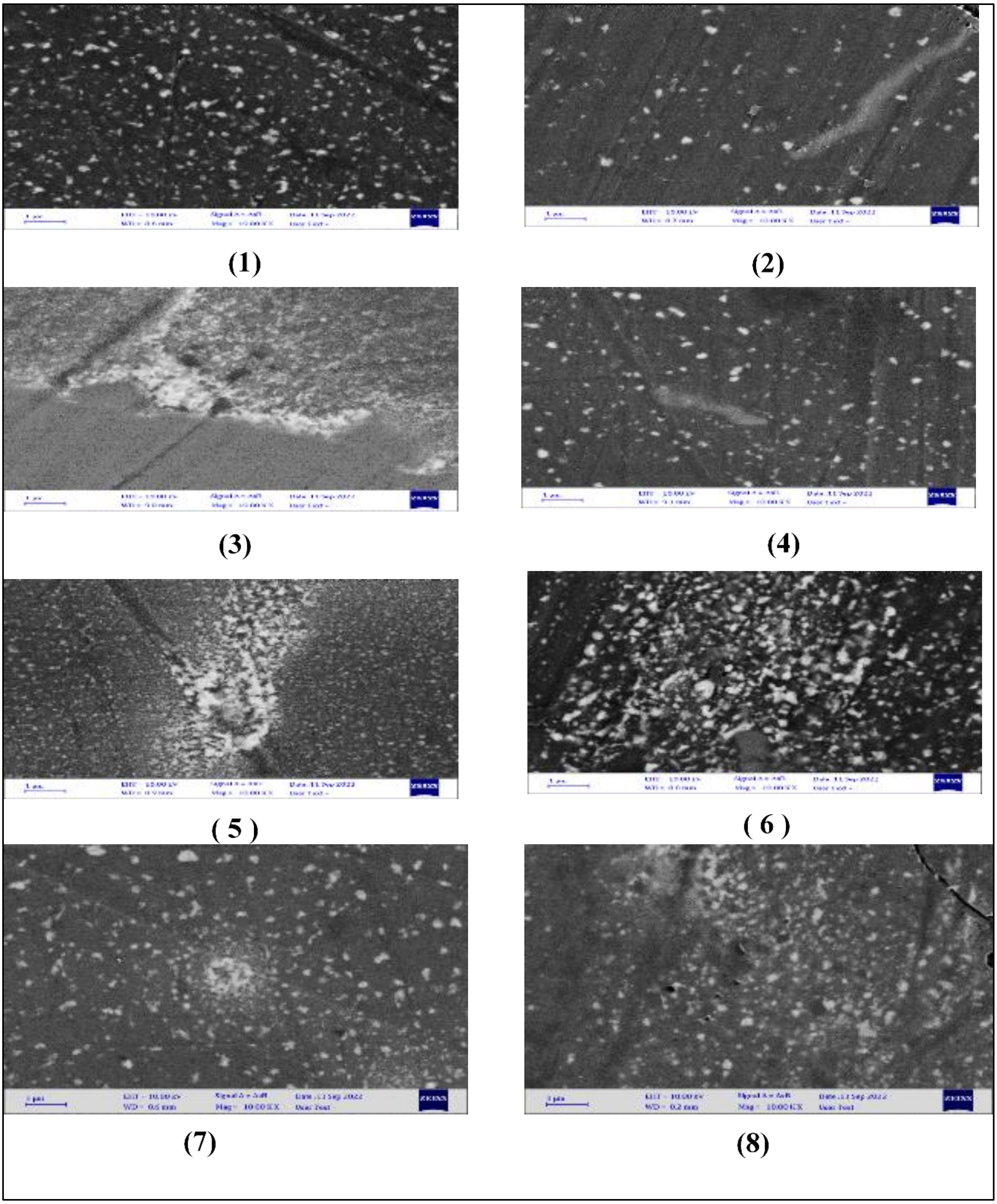

Figure 6 Scanning electron microscope (SEM)-Image from the longitudinal section in 1000× magnification of Al-Zn-Mn alloys; (1) AZM62 sample , (2) AZM61 sample, (3) AZM52 sample, (4) AZM51 sample , (5) AZM22 sample, (6) AZM21sample, (7) AZM4 sample, (8) AZM1 sample respectively

3.3.1. Hardness Measurement

For each of the alloys, the hardness has been measured. More specifically, HV, HB, and TS hardness determine have been performed. T The WOLPERT device of type (V-Testor 2) with P=1Kg has been used to determine the hardness of alloys. Equation (2) used to evaluate the HV. Using the HCT [11], the HB has been evaluated by equation (4). Equation (4) has been used to calculate the TS. Table (3) show the mechanical details and measurements for the all groups of alloy. According to the data in these tables, a correlation between the HV values and Al and Mg weights was found.

Table 3 Hardness measurement results of Al-Zn-Mn alloys

Code of alloys		Weight percent (% wt) (gm)			Hardness Measurement		
		Al	**Zn**	**Mn**	**HV (kg/mm^2)**	**HB (kg/mm^2)**	**TS (Mpa)**
1	AZM62	18	1	6	84.6	80.3	277
2	AZM61	18	1	6	61.94	58.8	202.8
3	AZM52	18	2	5	94.6	89.8	309.8
4	AZM51	18	2	5	41	38.9	134.2
5	AZM22	18	5	2	88	83.6	288.4
6	AZM21	18	5	2	101.7	96.6	333.3
7	AZM4	18	3	4	140	133	458.8
8	AZM1	18	6	1	88	83.6	288.4

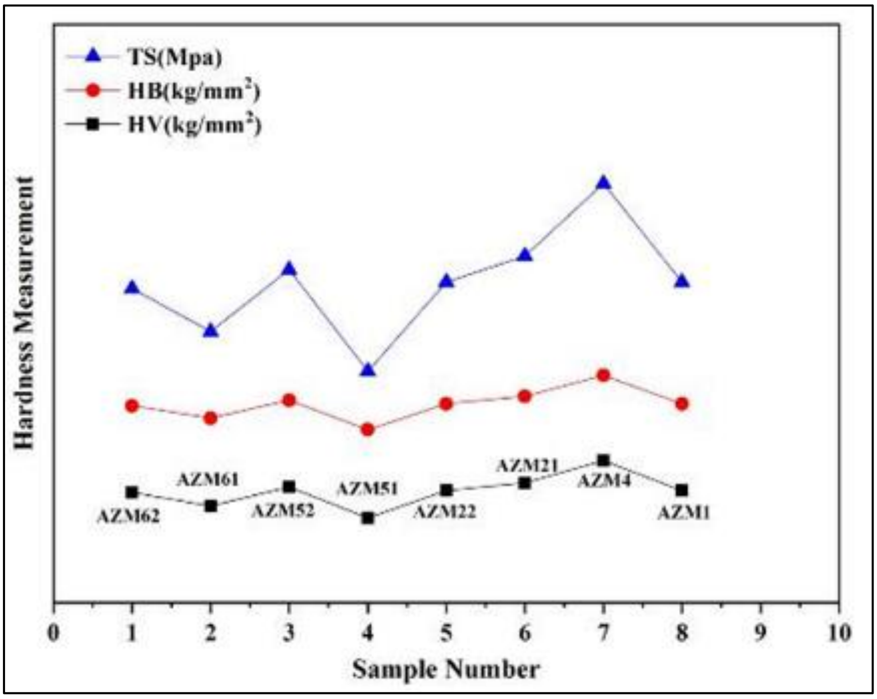

Figure 7 Hardness Measurement of alloys

The mechanical properties of Al-Zn-Mn alloys are shown in Figure (7), by compare the alloys, the alloy (AZM4) it's have maximum value of hardness. That means the Zn and Mn elements with together form a mechanically alloys. It shows that addition Zn and Mn to alloys to improve their mechanical properties. HV, HB, and TB all increase when Zn and Mn values increase. HV is improved from 88 kg/mm2 to 140 kg/mm2, HB is improved from 83.6 kg/mm^2 to 133 kg/mm^2, and TS is increased from 288.4 MP to 458.8 MP when Mn content increases from 1 to 4 wt%. While AZM61 alloy have 6% of Mn content, HV is 61.94 kg/mm^2, HB is 58.8 kg/mm^2 and TS is 202.8 MP. The tensile strength and tensile modulus of alloys significantly increase as the Mn element content increases.

4. Conclusion

These alloys have been produced by recycling aluminum wires that were used to transform electrical energy. To production of alloys were used the casting method aluminum wire with zinc and magnesium metals that high purity. The results of the EDS investigations, which are shown in Table 2, confirmed that the samples included a significant amount of aluminum and a low percentage of zinc metal. According to the microstructural analysis dendrites with micro precipitates were found in the α-Al matrix, All alloy have α-Al peak as main phase. Al_2Mn phase and $Al(MnZn)_6$ phase was considered as the secondary phase. As seen in Figure (6) of the SEM image, the presence of aluminum and manganese leads to the creation of Al2Mn components. The single-phase and two-phase zones, respectively, are shown by grey and black areas.The black zones were found to contain high significant Al and Mn element ratios. When comparing the alloys the mechanical characteristics of Al-Zn-Mn alloys, the alloy (AZM4) has the highest value of hardness. When Mn concentration increased from 1 to 4 wt%, HV increased from 88 kg/mm^2 to 140 kg/mm^2, HB increased from 83.6 kg/mm^2 to 133 kg/mm^2, and TS increased from 288.4 MP to 458.8 MP. As the Mn element content increases, the tensile strength and tensile modulus of alloys similarly increase significantly.

Compliance with ethical standards

Acknowledgments

The authors are grateful to the University of Mosul College of Science Department of Physics for their help.

Disclosure of conflict of interest

All the authors declare there are no conflicts of interest in connection with this paper, and the material described is not under publication or consideration for publication elsewhere.

References

[1] Kucharikova, L., Tillova, E., & Bokůvka, O. (2016). Recycling and properties of recycled aluminium alloys used in the transportation industry. Transport problems, 11(2), 117-122.

[2] Jirang, C. U. I., & Roven, H. J. (2010). Recycling of automotive aluminum. Transactions of Nonferrous Metals Society of China, 20(11), 2057-2063.

[3] Soo, V. K., Peeters, J., Paraskevas, D., Compston, P., Doolan, M., & Duflou, J. R. (2018). Sustainable aluminium recycling of end-of-life products: A joining techniques perspective. Journal of Cleaner Production, 178, 119-132.

[4] Wang, H. Z., Leung, D. Y., Leung, M. K. H., & Ni, M. (2009). A review on hydrogen production using aluminum and aluminum alloys. Renewable and sustainable energy reviews, 13(4), 845-853.

[5] Lamberti, M., & Escher, F. Aluminium foil as a food packaging material in comparison with other materials. Food Reviews International. (2007); 23(4)407-433.

[6] Gronostajski, J., Marciniak, H., & Matuszak, A. New methods of aluminium and aluminium-alloy chips recycling. Journal of materials processing technology.(2000); 106(1-3): 34-39.

[7] Callister Jr, W. D., & Rethwisch, D. G.Fundamentals of materials science and engineering an integrated approach.(2020); John Wiley & Sons.

[8] Salih, S. E., & Al-Jnabi, M. M.Study of Mechanical Properties of (Al-Cu-Mg) Alloy Matrix Composite. Al-Khwarizmi Engineering Journal. (2012); 8(3):95-107.

[9] Al-Nima, R. R. O., & Al-jiboori, M. A. H. (2021). Manufacturing Al-Cu-Mg Alloys and Studying Various Mechanical Properties. Advances in Mechanics, 9(3), 291-311.

[10] Moreira, F. D. L., Kleinberg, M. N., Arruda, H. F., Freitas, F. N. C., Parente, M. M. V., de Albuquerque, V. H. C., & Rebouças Filho, P. P.A novel Vickers hardness measurement technique based on Adaptive Balloon Active Contour Method. Expert systems with applications. (2016); (2016);45:294-306.

[11] Chen, J., Chen, Z., Yan, H., Zhang, F., & Liao, K. Effects of Sn addition on microstructure and mechanical properties of Mg–Zn–Al alloys. Journal of Alloys and Compounds. (2008); 461(1-2):209-215.

[12] Wolverton, C. J. A. M. Crystal structure and stability of complex precipitate phases in Al–Cu–Mg–(Si) and Al–Zn–Mg alloys. Acta Materialia. (2001); 49(16):3129-3142.

[13] Hu, G. S., Zhang, D. F., Zhao, D. Z., Xia, S. H. E. N., Jiang, L. Y., & Pan, F. S. Microstructures and mechanical properties of extruded and aged Mg–Zn–Mn–Sn–Y alloys. Transactions of Nonferrous Metals Society of China .(2014); 24(10):3070-3075.

[14] Liaw, L. L., & Yusuf, N. K.A Review on Aluminum Alloy Recycling Technique. Research Progress in Mechanical and Manufacturing Engineering. (2022). 3(1):175-183.